中國機械工程學刊第三十九卷第一期第 53~63 頁(民國一百零七年)
Journal of the Chinese Society of Mechanical Engineers, Vol.39, No.1, pp 53~63 (2018)

Cyclic Bending Deterioration and Failure of Locally-dented Circular Tubes

Kuo-Long Lee*, Chen-Cheng Chung** and Wen-Fung Pan***

Keywords： cyclic bending deterioration, cyclic bending failure, local-dented circular tubes, finite element analysis.

ABSTRACT

In this paper, we present an experiment and an analysis method for inspecting the deterioration and failure of locally-dented 6061-T6 aluminum alloy tubes under cyclic bending. A simple technique was employed to produce small transverse local dents on the tubes. Tubes with dent depths varying from very shallow to approximately 2.4 times the tube wall thickness were considered. The ovalization-curvature curve showed an increase in asymmetry and ratcheting with an increase in the number of bending cycles. Deeper dent depths caused larger ovalization. Tubes with five different dent depths were tested. The relationship between the controlled curvature and number of bending cycles required to produce failure on a log-log scale exhibited five nonparallel straight lines. Finally, a finite element model was used to describe the moment-curvature and ovalization-curvature relationship. In addition, an empirical formula was suggested to simulate the relationship between the controlled curvature and number of bending cycles required to produce failure. It was found that the experimental and analytical data agreed well.

INTRODUCTION

It is well known that the bending of circular tubes results in ovalization (change in the outer diameter divided by the original outer diameter) of the tube cross-section. This ovalization increases slowly during reverse bending and continuous cyclic bending, and in turn, results in the deterioration of the circular tube, which buckles or fractures when the ovalization reaches a critical value. Circular tubes are severely damaged during buckling and fracturing and can't bear the load, which ultimately results in obstruction and leakage of the material being transported. As such, a complete understanding of the deterioration and failure of circular tubes under cyclic bending is essential for industrial application.

As part of the earliest research on this issue, Kyriakides' team began a series of experimental and theoretical studies on tubes subjected to monotonic and cyclic bending, as well as with and without external or internal pressure. Shaw and Kyriakides (1985) investigated the elastic-plastic response of thin-walled tubes under cyclic bending. They showed a gradual increase in the tube's ovalization during reverse and continuous cyclic bending. Corona and Kyriakides (1991) experimentally investigated the weakening and failure of tubes under cyclic bending with external pressure. In their research, the effects of the cyclic bending path with and without external pressure on the ovalization accumulation rate and the timing of buckling were examined. Furthermore, Corona and Kyriakides (2000) investigated the failure of tubes subjected to bending with and without external pressure. Asymmetric imperfections and buckling were theoretically evaluated with a previously derived formula. Similarly, Corona et al. (2006) discovered that such tubes display plastic anisotropy and described this using Hill's yield criterion. By including the material anisotropy, they evaluated prebuckling, postbuckling, and bifurcation using flow and deformation theories. Limam, et al. (2012) investigated the failure of locally-dented tubes under pure bending with internal pressure. Using finite element models, the dent production, tube pressurization, and tube bending for collapse were properly described. Bechle and Kyriakides (2014) examined the localization of NiTi tubes subjected to bending. The influence of the texture and material asymmetry on the tube structure was studied.

In addition, other scholars have published a number of related research papers. Yuan and Mirmiran (2001) experimentally and theoretically examined the collapse of fiber-reinforced plastic tubes filled with concrete and subjected to bending. Elchalakani et al. (2002) tested grade C350 steel

Paper Received May, 2016. Revised September, 2016, Accepted October, 2016, Author for Correspondence: Wen-Fung Pan.

**Professor, Department of Innovative Design and Entrepreneurship Management, Far East University, Tainan, Taiwan 744, ROC.*

***Gradnate Student, Department of Engineering Science, National Cheng Kung University, Tainan, Taiwan 701, ROC.*

****Professor, Department of Engineering Science, National Cheng Kung University, Tainan, Taiwan 701, ROC.*

tubes with different diameter-to-thickness ratios (D_o/t ratios) under pure bending. Jiao and Zhao (2004) experimentally investigated the plastic slenderness limit of very-high-strength circular steel tubes under bending. Houliara and Karamanos (2006) studied the buckling and postbuckling of thin-walled tubes under in-phase bending and internal pressure. Mathon and Liman (2006) experimentally studied the collapse of thin-walled tubes subjected to pure bending and internal pressure. Elchalakani and Zhao (2008) investigated the response of concrete-filled, cold-formed circular steel tubes subjected to monotonic and cyclic bending with variable amplitudes. Suzuki et al. (2010) examined the response of local buckling for 48 high-strain line pipes under pure bending. Zhi et al. (2012) studied the instability and failure of single-layer, cylindrical, reticulated tubes subjected to earthquake motion. Guo et al. (2013) discussed the response of thin-walled circular tubes with a hollow subjected to bending.

Pan et al. (1998) designed and set up a new measurement apparatus. The apparatus was used with a cyclic bending machine to study various types of tube under different cyclic bending conditions. For example: Pan and Fan (1998) studied the effect of the prior curvature rate at the preloading stage on subsequent creep (moment is kept constant for a period of time) and relaxation (curvature is kept constant for a period of time). Pan and Her (1998) investigated the response and stability of 304 stainless steel tubes subjected to cyclic bending at different curvature rates. Lee et al. (2001) studied the influence of the D_o/t ratio on the response and stability of circular tubes subjected to symmetrical cyclic bending. Lee et al. (2004) experimentally explored the effect of the D_o/t ratio and curvature rate on the response and stability of circular tubes subjected to cyclic bending. Chang et al. (2008) studied the mean moment effect on circular, thin-walled tubes under cyclic bending. Chang and Pan (2009) discussed the buckling life estimation of circular tubes subjected to cyclic bending.

Tubes are typically used in harsh environments, which may corrode the surfaces and create notches. Notched tubes should exhibit responses and collapse mechanisms different from their smooth-surfaced counterparts. From 2010, Pan's research group started experimental and theoretical investigations on the response of sharp-notched tubes under cyclic bending. Lee et al. (2010) experimentally examined the change in ovalization along with the number of bending cycles for sharp-notched circular tubes subjected to cyclic bending. Three stages (initial, secondary, and tertiary) were clearly observed from the curve of ovalization versus the number of bending cycles. Later, Lee (2010) investigated the behavior and failure of 304 sharp-notched stainless steel tubes subjected to cyclic bending. Asymmetry, ratcheting, and increasing ovalization-curvature curves were discovered. In addition, Lee et al. (2013) experimentally examined the viscoplastic buckling of 304 sharp-notched stainless steel circular tubes under cyclic bending, and changes in both the notch depth and curvature rate were examined. Observations of a certain curvature rate revealed that the cyclic-controlled curvature and the number of bending cycles required to yield buckling relationships at a log–log scale exhibited parallel lines for every notch depth. However, all investigations were performed on the circumferential sharp notch as shown in Fig. 1.

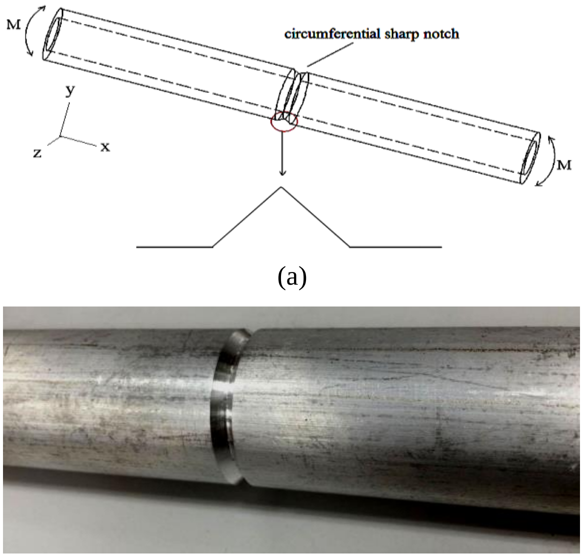

(a)

(b)

Fig. 1. (a) A schematic drawing and (b) picture of the circumferential sharp-notched circular tube.

External impact or pressure during transportation, erection, or use, will cause the tube to dent. The dent depth is either very shallow or is likely to exceed the wall thickness. When a tube with a dent is subjected to cyclic bending, the behavior and failure are different from that of a tube with a smooth surface or a notch. In 2012, Limam et al. (2012) experimentally and analytically inspected the collapse curvature of locally-dented tubes subjected to pure bending with internal pressure. In their experiments, 321 stainless steel tubes with outer diameters of 1.5 in. and D_o/t of 52 were tested. The dented tubes were internally pressurized and then bent to collapse. They found that such defects decreased the bending rigidity quite significantly. In addition, finite element models were employed to simulate the denting on tubes, internal pressurization, and bending to collapse. Although Limam et al. were the first to study locally-dented tubes under bending, they used monotonic bending. It is well known that the response of a tube subjected to monotonic bending is different from that of a tube subjected to cyclic bending. Moreover, types of failure are also different for the two loadings, and the number of bending cycles required for failure is a very important quantity for tubes subjected to cyclic bending. Therefore, the deterioration and failure of locally-dented circular tubes subjected to cyclic bending are investigated here.

In this paper, locally-dented 6061-T6 aluminum alloy tubes with different dent depths under cyclic bending were experimentally studied. Related experimental tests were conducted using a tube-bending machine and curvature-ovalization measurement apparatus. The bending moment, curvature, and ovalization were measured with sensors at the testing facility. The number of bending cycles required to produce failure was also recorded

EXPERIMENTS

By using a tube-bending device and a curvature-ovalization measurement apparatus, locally-dented circular tubes with different dent depths and subjected to cyclic bending were studied in this paper. The experimental device, materials, specimens, and test procedures are detailed below.

Experimental Device

The experiments were performed in a specially-built testing facility, shown schematically in Fig. 2(a). This was designed to perform bending, reverse, and cyclic tests. A detailed explanation of the experimental facility can be found in many papers (Pan and Her (1998), Lee et al. (2001)). Fig. 2(b) schematically shows the light-weight instrument designed by Pan et al. (1998) for measuring the curvature and ovalization of a tube. The angle variation during cyclic bending can be measured by two side-inclinometers in the instrument. The tube curvature can be obtained by a simple calculation, i.e., an extended version of the calculation described by Pan et al. (1998).

Material and Specimens

6061-T6 aluminum alloy tubes were used for the experiment. The chemical composition of the tested material is given in Table 1. The mechanical properties were as follows: ultimate stress of 258 MPa, 0.2% strain offsetting yield stress of 166 MPa, and percent elongation of 23%.

Table 1. Chemical composition of 6061-T6 aluminum alloy (weight %).

Chemical Composition	Al	Mg	Si	Ti	Fe
Proportion (%)	98.096	0.937	0.535	0.012	0.139
Chemical Composition	Mn	Zn	Cr	Ni	
Proportion (%)	0.022	0.0983	0.022	0.005	

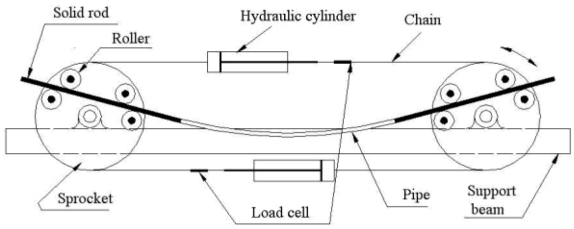

(a)

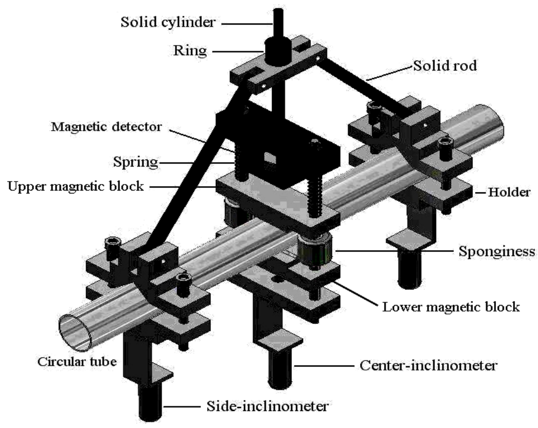

(b)

Fig. 2. (a) A schematic drawing of the bending device and (b) schematic drawing of the curvature-ovalization measurement apparatus.

The outer surfaces of the original tubes with D_o = 35.0 mm and t = 3.0 mm were processed to introduce the expected dents. Figs. 3(a) and 3(b) show a picture and a schematic drawing of dent production, respectively. The upper mold made contact with the tube surface and exerted a pressure to create the dent. In this study, five dent depths (a) were considered: 0.0, 0.3, 0.6, 0.9, and 1.2 mm. Note that a = 0.0 mm represents a tube with a smooth surface. Figs. 4(a) and 4(b) show a picture and a schematic drawing of a locally-dented tube with a = 1.2 mm. In addition, the experimental data were normalized using actual geometric and material parameters. The bending moment and tube curvature were normalized using $M_o(\sigma_o D_o^2 t)$ and $\kappa_o(t/D_o^2)$, respectively (Corona and Kyriakides (1988)).

(a)

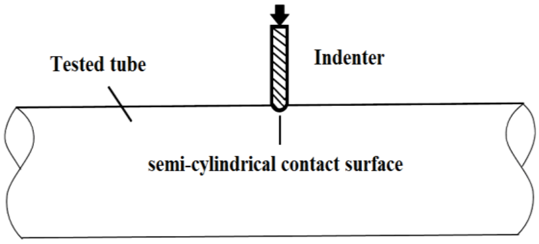

(b)

Fig. 3. (a) A picture and (b) schematic drawing of processing a dent on the 6061-T6 aluminum alloy tube.

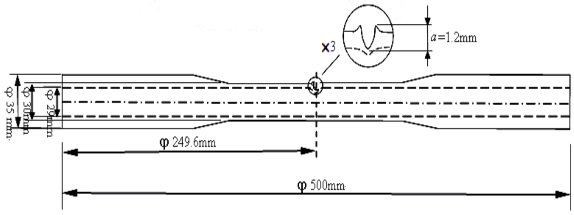

(a)

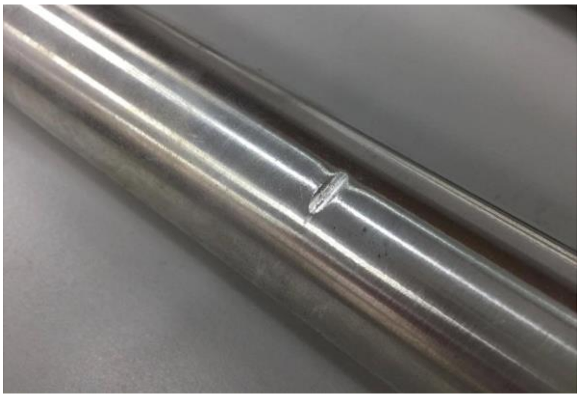

(b)

Fig. 4. (a) A picture and (b) schematic drawing of a local-dented 6061-T6 aluminum alloy tube with a = 1.2 mm.

FINITE ELEMENT ANALYSIS

In this study, the response of locally-dented circular tubes subjected to cyclic bending was also analyzed numerically using the finite element code ANSYS. The response is the correlation among the moment, curvature, and ovalization. The elastic-plastic stress-strain response, model, mesh, boundary conditions, and loading conditions are explained below.

Elastic-plastic Stress-strain Curves

Fig. 5 shows the tested and ANSYS-constructed uniaxial stress (σ) - strain (ε) curves for the 6061-T6 aluminum alloy. The kinematic hardening rule was used as the hardening rule for cyclic loading.

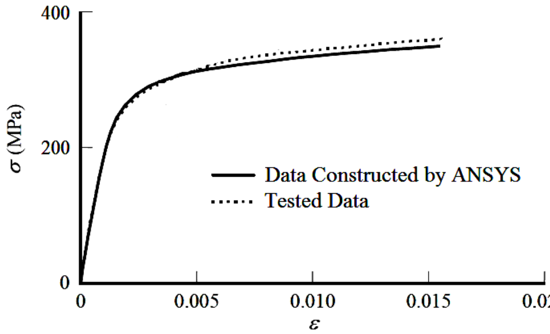

Fig. 5. Tested and ANSYS constructed data of the uniaxial stress (σ) - strain (ε) curve for 6061-T6 aluminum alloy.

Model

The model consisted of three parts: the locally-dented tube, the indenter, and the solid rod. The size and geometric shape of the locally-dented tube are stated in a previous section and the schematic drawings of the indenter and solid rod are shown in Figs. 6(a) and 6(b), respectively. It can be seen in Fig. 6(a) that production of a dent includes the indenter and a fixed plate. The indenter exerts a pressure on the tube related to the desired depth of the dent. The shape and size of the dents are discussed in a previous section.

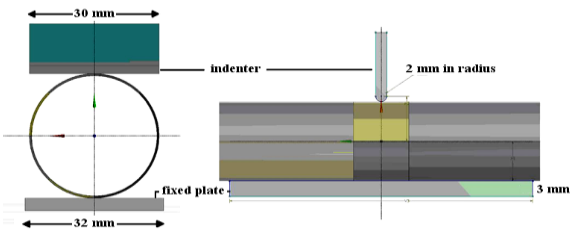

(a)

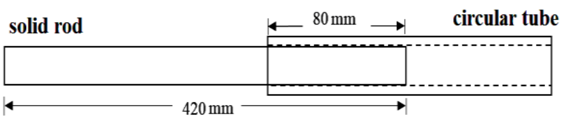

(b)

Fig. 6. Schematic drawings of (a) the indenter and (b) solid rod.

Mesh

Due to the three-dimensional geometry and elastic-plastic deformation of the tube, the SOLID 185 element was used for relative analysis. This is a tetrahedral element built in ANSYS and is suitable for analyzing plastic or large deformations. In particular, the element can adequately analyze shell components under bending. Due to the right and left symmetry, only half of the tube model was constructed. Fig. 7(a) shows the mesh constructed by ANSYS for the indenter and half tube, and Fig. 7(b) shows the mesh constructed by ANSYS for the half tube.

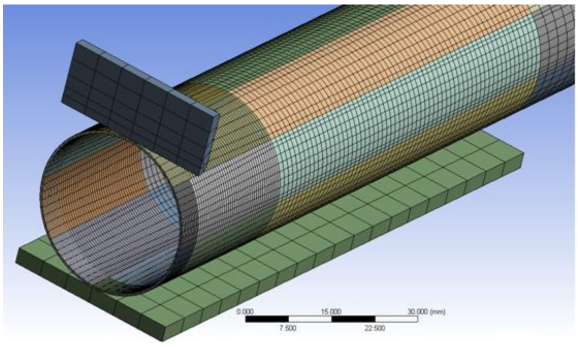

(a)

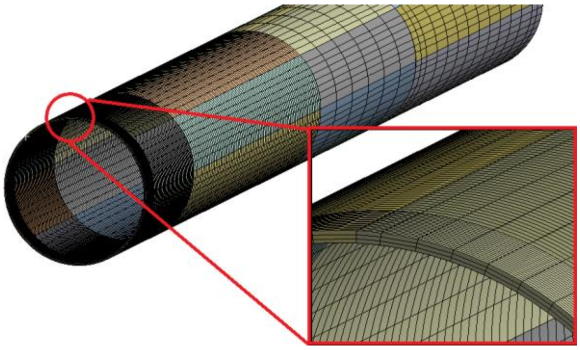

(b)

Fig. 7. Mesh constructed by ANSYS for (a) the indenter and (b) half tube.

Boundary Conditions

When producing a local dent on the tube, the indenter moved in the y-direction only. Therefore, friction supports were set to prevent any displacement in the x- or z-directions, as shown in Fig. 8(a). The indenter was set to exert pressure on the tube to produce a dent and then to reset back to its original position. The contact between the indenter and tube was set to be frictionless, as shown in Fig. 8(b). The plate was fixed, thus, a fixed support was set on the plate as shown in Fig. 9(a). As there was no related displacement between the tube and the fixed plate, the bonded contact between them was used, as shown in Fig. 9(b).

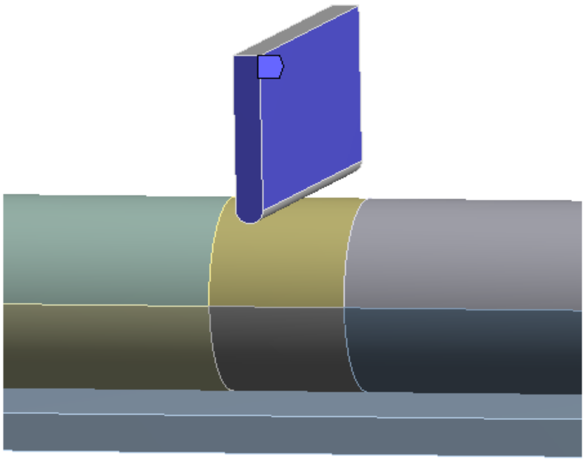

(a)

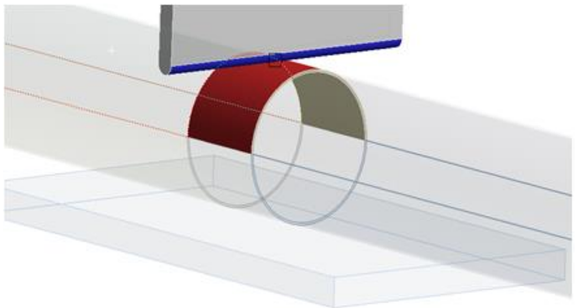

(b)

Fig. 8. Boundary conditions for (a) the indenter and (b) contact between the indenter and tube.

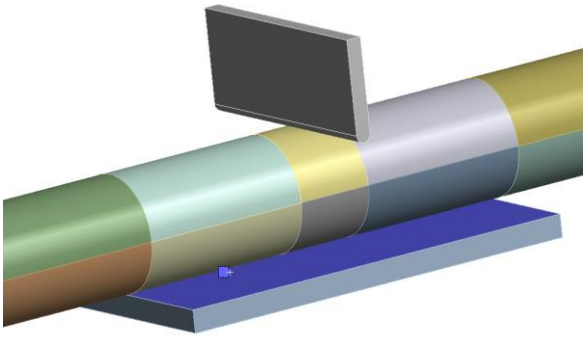

(a)

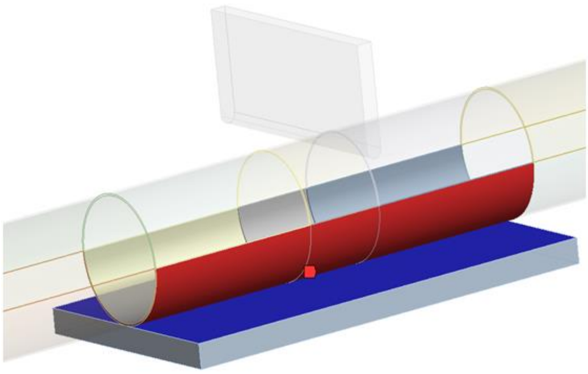

(b)

Fig. 9. Boundary conditions for (a) the fixed plate and (b) contact between the tube and fixed plate.

Loading Conditions

When producing a dent, the indenter was set to move downward to create a desired dent depth, then travel back to its original position. Fig. 10(a) shows the loading conditions of the indenter as constructed by ANSYS. Fig. 10(b) shows the loading condition constructed by ANSYS on the basis of the tube-bending device. As shown, the remote displacement of the solid rod in the z-direction was unrestricted, i.e., the rotation was free to move in the z-direction. In addition, the bending moment was applied only in the z-direction, hence, the rotations in the x- and y-directions were set to zero.

Fig. 11 depicts a tube subjected to pure bending. The rotating angle θ was used as input data for curvature-controlled cyclic bending. The curvature κ is

$$\kappa = 1/\rho = 2\theta/L_o, \quad (1)$$

where ρ is the radius of curvature and L_o is the original tube length.

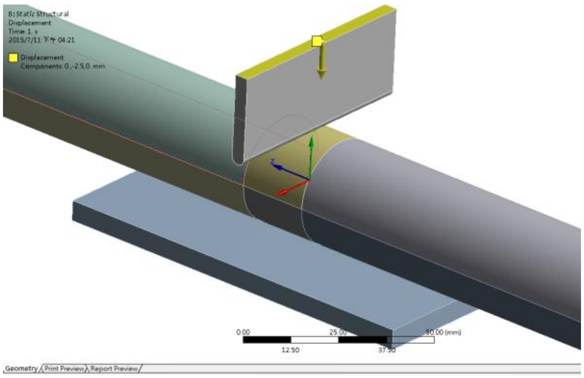

(a)

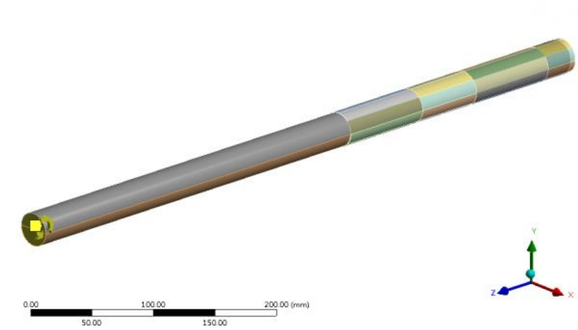

(b)

Fig. 10. Loading conditions for (a) the indenter and (b) solid rod.

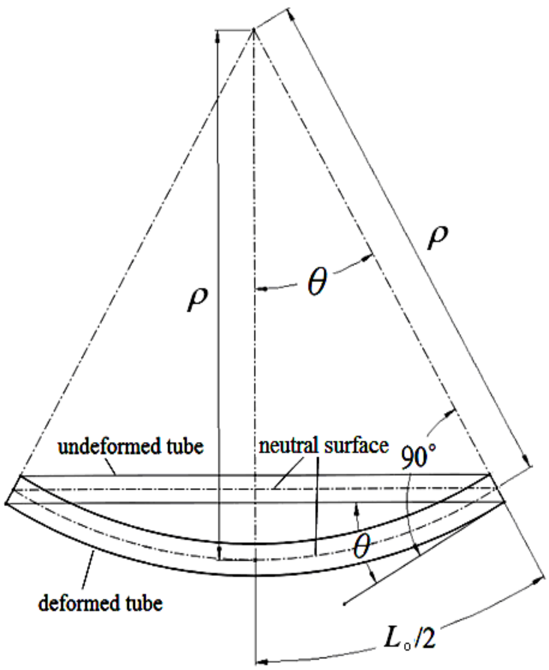

Fig. 11. Relationship between θ and κ for a tube under pure bending.

COMPARISON BETWEEN EXPERIMENTAL AND SIMULTED RESULTS

Response of Locally-dented 6061-T6 Aluminum Alloy Tubes with Different Dent Depths under Cyclic Bending

A typical set of experimental relationships between moment (M/M_o) and curvature (κ/κ_o) for locally-dented 6061-T6 aluminum alloy tubes with different a subjected to cyclic bending is shown in Figs. 12(a)-(e). The tubes were cycled between $\kappa/\kappa_o = \pm 0.71$. It can be seen that the M/M_o-κ/κ_o relationships for different a are nearly closed and steady hysteresis loops. The magnitudes of M/M_o are almost equal to each other at κ/κ_o = +0.71 and κ/κ_o = −0.71 for smooth tubes (a = 0.0 mm). For dented tubes ($a \neq 0.0$ mm), due to the contact of the two sides of the dent during reverse bending, the magnitude of M/M_o at κ/κ_o = −0.71 is smaller than that at κ/κ_o = +0.71. But, the M/M_o-κ/κ_o curves are almost the same when $a \geq 0.6$ mm. This characteristic of the M/M_o-κ/κ_o response is different from that obtained by Lee et al.

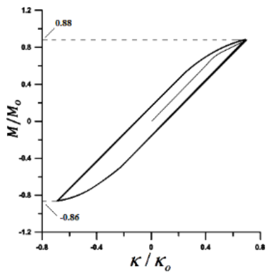

(a)

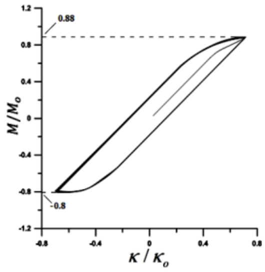

(b)

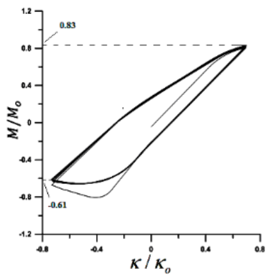

(c)

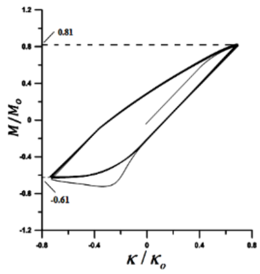

(d)

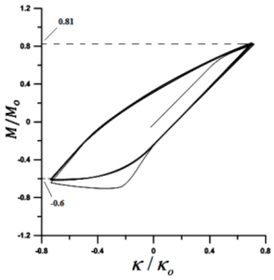

(e)

Fig. 12. Experimental moment (M/M_o) - curvature (κ/κ_o) curves for locally-dented 6061-T6 aluminum alloy tubes with a = (a) 0.0, (b) 0.3, (c) 0.6, (d) 0.9

and (e) 1.2 mm under cyclic bending.

(2010), and Lee et al. (2013) for sharp-notched SUS304 stainless steel tubes. They discovered that the M/M_o-κ/κ_o response became stable after a few bending cycles. The M/M_o-κ/κ_o loops looked similar for different values of a. In addition, tubes with a higher a represented a smaller t, therefore, a lower moment was needed to bend the tube to a desired curvature. Figs. 13(a)-(e) show the corresponding M/M_o-κ/κ_o curves simulated by ANSYS.

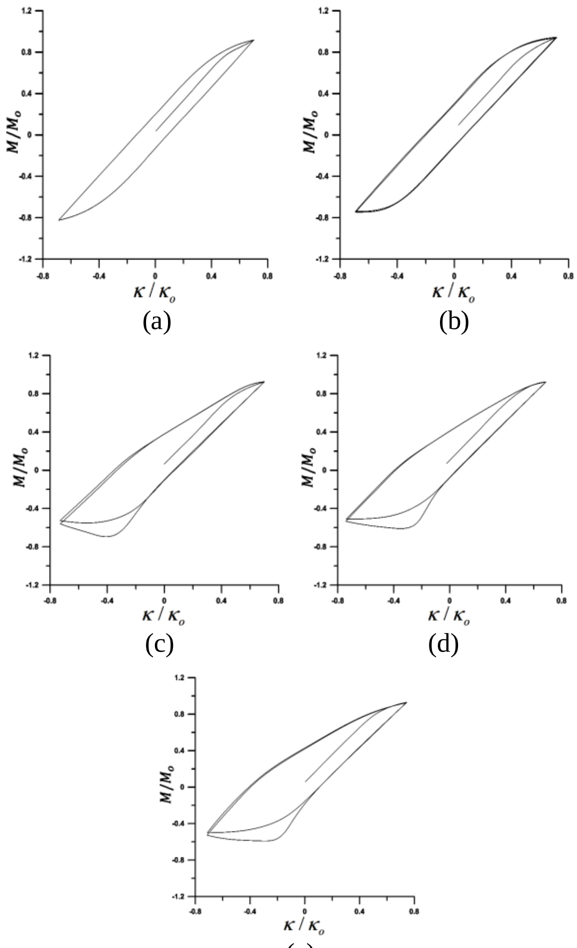

Fig. 13. ANSYS simulated moment (M/M_o) - curvature (κ/κ_o) curves for locally-dented 6061-T6 aluminum alloy tubes with a = (a) 0.0, (b) 0.3, (c) 0.6, (d) 0.9, and (e) 1.2 mm under cyclic bending.

The corresponding set of ovalization ($\Delta D_o/D_o$) - curvature (κ/κ_o) relationships are shown in Figs. 14(a)-(e). It is noted that the $\Delta D_o/D_o$-κ/κ_o curves exhibit a ratcheting trend and increase with the number of bending cycles. A larger a results in a more asymmetrical look to the $\Delta D_o/D_o$-κ/κ_o curve. Moreover, larger a of dented tubes leads to larger ovalization. This characteristic of the $\Delta D_o/D_o$-κ/κ_o response is similar to that obtained by Lee et al. (2010), Lee (2010), and Lee et al. (2013) for sharp-notched SUS304 stainless steel tubes. Due to differing materials, sizes, and types of defect, the increase in $\Delta D_o/D_o$ for sharp-notched SUS304 stainless steel tubes is much small than that for locally-dented 6061-T6 aluminum alloy tubes. Figs. 15(a)-(e) demonstrate the corresponding ANSYS simulated $\Delta D_o/D_o$-κ/κ_o curves for Figs. 14(a)-(e), respectively.

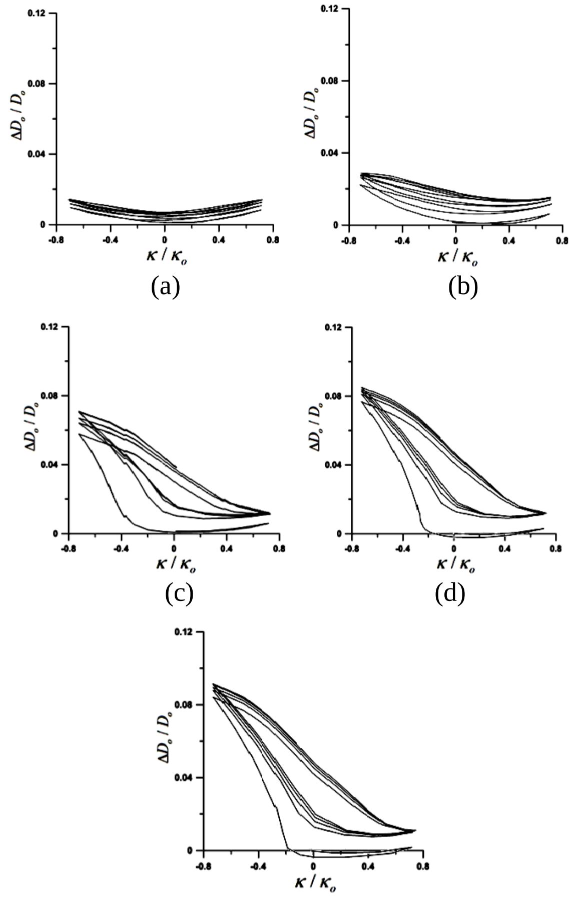

Fig. 14. Experimental ovalization ($\Delta D_o/D_o$) - curvature (κ/κ_o) curves for locally-dented 6061-T6 aluminum alloy tubes with a = (a) 0.0, (b) 0.3, (c) 0.6, (d) 0.9, and (e) 1.2 mm under cyclic bending.

Failure of Locally-dented 6061-T6 Aluminum Alloy Tubes with Different Dent Depths under Cyclic Bending

The experimental data of cyclic curvature (κ_c/κ_o) versus the number of bending cycles required to produce failure (N_f), for locally-dented 6061-T6 aluminum alloy tubes submitted to cyclic bending with different a, is illustrated in Fig. 16(a). For a fixed curvature, tubes with a larger a cause lower N_f. Next, the experimental data in Fig. 16(a) were plotted on a log-log scale and five non-parallel straight lines resulted, Fig. 16(b). Note that the lines were least square fits of the data. This result is different from that obtained by Lee (2010) and Lee et al. (2013) for sharp-notched SUS304 stainless steel tubes. They discovered parallel straight lines for κ_c/κ_o-N_f

relationships on a log-log scale for every notch depth.

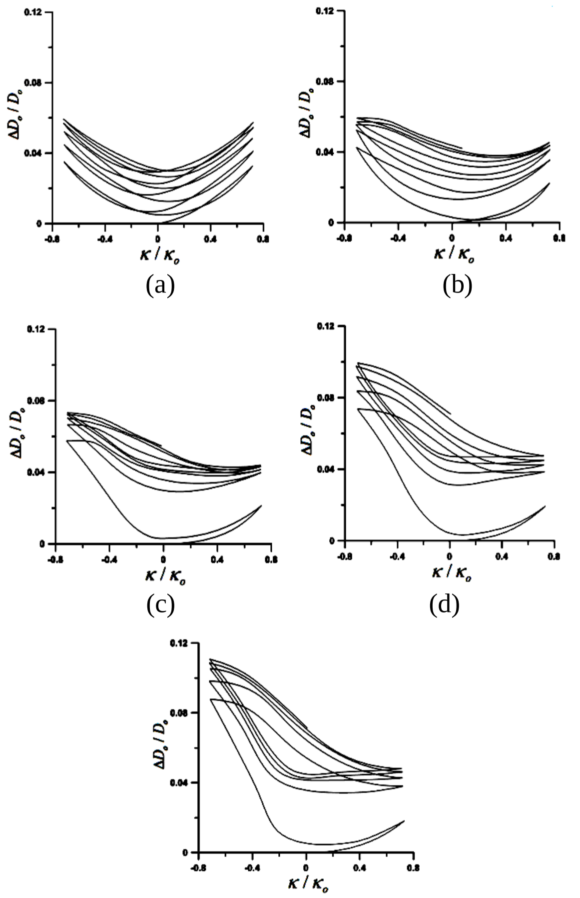

Fig. 15. ANSYS simulated ovalization ($\Delta D_o/D_o$) - curvature (κ/κ_o) curves for locally-dented 6061-T6 aluminum alloy tubes with a = (a) 0.0, (b) 0.3, (c) 0.6, (d) 0.9, and (e) 1.2 mm under cyclic bending.

In 1987, Kyriakides and Shaw (1987) suggested a formula to describe the relationship between κ_c/κ_o and the number of bending cycles required to produce buckling (N_b):

$$\kappa_c/\kappa_o = C\,(N_b)^{-\alpha} \tag{2a}$$

or

$$\log \kappa_c/\kappa_o = \log C - \alpha \log N_b, \tag{2b}$$

where C and α are the material parameters. Since the failure types in our study were buckling for a = 0.0 mm and fracture for $a \neq$ 0.0 mm, formula (2) was modified to

$$\kappa_c/\kappa_o = C\,(N_f)^{-\alpha} \tag{3a}$$

or

$$\log \kappa_c/\kappa_o = \log C - \alpha \log N_f, \tag{3b}$$

where C is the value of κ_c/κ_o by letting $N_f = 1$, and α is the slope of the line in the log-log plot. Based on the experimental data in Fig. 16(b), five values of C and α were obtained for a = 0.0, 0.3, 0.6, 0.9, and 1.2 mm from Eq. (3b), as shown in Table 2.

Table 2. Experimental determined C and α for different a.

a (mm)	0.0	0.3	0.6	0.9	1.2
a/t	0.0	0.6	1.2	1.8	2.4
C	0.936	0.864	0.756	0.684	0.630
α	0.106	0.118	0.133	0.142	0.164

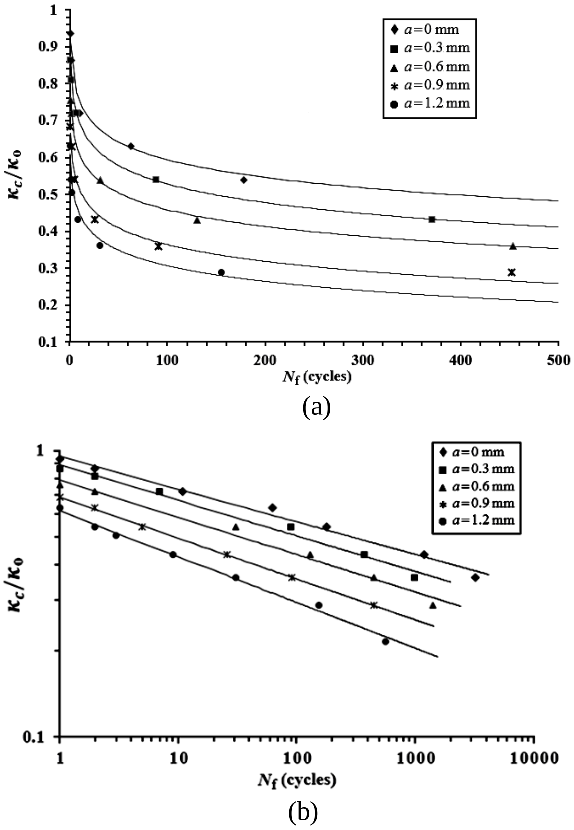

Fig. 16. Experimental cyclic curvature (κ/κ_o) versus the number of bending cycles required to produce failure (N_f) for locally-dented 6061-T6 aluminum alloy tubes with different a on (a) decimal and (b) double logarithmic coordinates.

By considering the linear distribution of the experimental relationship between $\ln C$ and a/t in Fig. 17(a), the following formulation was proposed

$$\ln C = C_o - \beta\left(\frac{a}{t}\right), \tag{4}$$

where C_o and β are material parameters. From Fig. 17(a), C_o and β were determined to be -0.067 and 0.17, respectively. By observing the linear distribution of the experimental relationship between

$\ln\alpha$ and a/t in Fig. 17(b), the following formulation was proposed

$$\ln\alpha = \alpha_o - \gamma\left(\frac{a}{t}\right), \tag{5}$$

where α_o and γ are material parameters. From Fig. 17(b), α_o and γ were determined to be -2.24 and -0.18, respectively. Finally, the simulated result of the cyclic curvature (κ_c/κ_o) versus the number of bending cycles required to produce failure (N_f) in locally-dented 6061-T6 aluminum alloy tubes with different a under cyclic bending was determined using Eqs. (3), (4), and (5) is demonstrated in Fig. 18. It can be seen that the simulated result correlates well with the experimental findings.

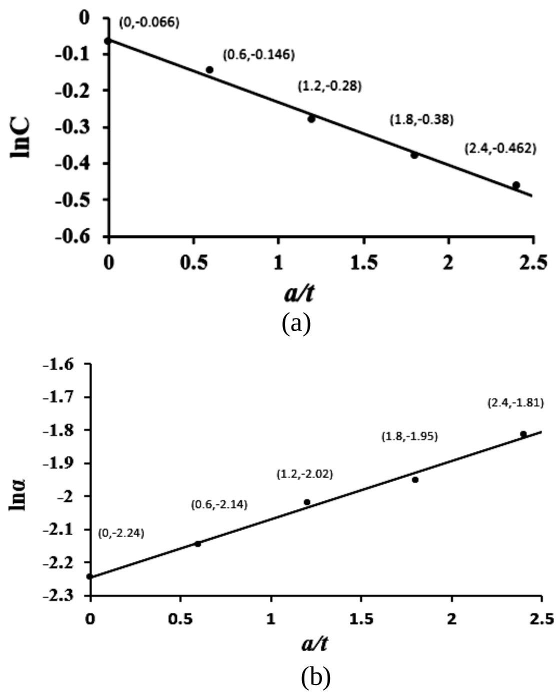

(b)

Fig. 17. Relationships (a) between ln$C$ and a/t and (b) between lnα and a/t.

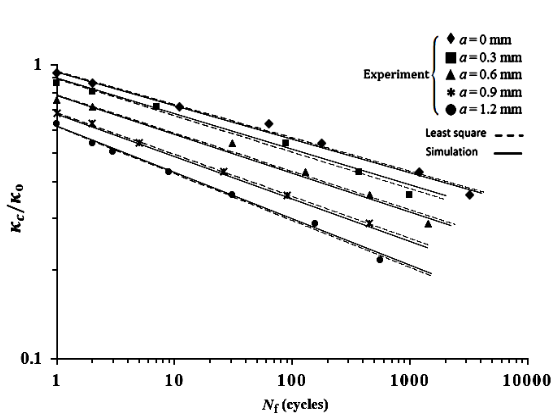

Fig. 18. Experimental and simulated cyclic curvature (κ/κ_o) versus the number of cycles required to failure (N_f) for locally-dented 6061-T6 aluminum alloy tubes with different a on double logarithmic coordinates.

CONCLUSIONS

The deterioration and failure of locally-dented 6061-T6 aluminum alloy tubes, with different a and submitted to cyclic bending, were investigated. As a result of the experimental and simulated results, some important conclusions have been reached and are presented as follows:

(1) Under symmetrical cyclic bending, the experimental M/M_o-κ/κ_o relationship for locally-dented 6061-T6 aluminum alloy tubes with any a exhibits a closed and stable hysteresis loop. In addition, the magnitudes of M/M_o are almost equal at the maximum and minimum curvatures for a = 0.0 mm. Due to the two sides of the dent coming into contact during reverse bending, the magnitude of M/M_o at the minimum curvature is smaller than at the maximum curvature.

(2) Under symmetrical cyclic bending, the experimental $\Delta D_o/D_o$-κ/κ_o relationship for locally-dented 6061-T6 aluminum alloy tubes with any a exhibits an increase and ratcheting with an increase in the number of bending cycles. The $\Delta D_o/D_o$-κ/κ_o curves are symmetrical for a = 0.0 mm and asymmetrical for $a \neq$ 0.0 mm. In addition, larger a causes more asymmetry and larger ovalization.

(3) By employing the proper stress-strain relationship, model, mesh, boundary conditions, and loading conditions, ANSYS can describe the behavior of locally-dented circular tubes under cyclic bending. The experimental moment-curvature and ovalization-curvature relationships were compared with the ANSYS simulation. Good agreement between the simulated and experimental results was achieved.

(4) The formula, Eq. (2), suggested by Kyriakides and Shaw (1987) was modified to simulate the κ/κ_o-N_f relationship for locally-dented 6061-T6 aluminum alloy tubes with different a subjected to cyclic bending. Based on the experimental data, the formulation of the material parameters C and α are proposed in Eqs. (4) and (5), respectively. It can be seen that the simulated results are in good agreement with the experimental findings, as shown in Fig. 18.

ACKNOWLEDGEMENT

The research was executed with the support of the Ministry of Science and Technology under grant MOST 103-2221-E-006-041. We sincerely thank them for their assistance.

REFERENCES

Bechle, N.J., and Kyriakides, S., "Localization of NiTi Tubes under Bending," *Int. J. Solids Struct.*, Vol. 51, No. 5, pp. 967-980 (2014).

Chang, K.H., and Pan, W.F., "Buckling Life Estimation of Circular Tubes under Cyclic Bending," *Int. J. Solids Struct.*, Vol. 46, No. 2, pp. 254-270 (2009).

Chang, K.H., Pan, W.F., and Lee, K.L., "Mean Moment Effect of Thin-walled Tubes under Cyclic Bending," *Struct. Eng. Mech.*, Vol. 28, No. 5, pp. 495-514 (2008).

Corona, E., and Kyriakides, S., "On the Collapse of Inelastic Tubes under Combined Bending and Pressure," *Int. J. Solids Struct.*, Vol. 24, No. 5, pp. 505-535 (1988).

Corona, E., and Kyriakides, S., "An Experimental Investigation of the Degradation and Buckling of Circular Tubes under Cyclic Bending and External Pressure," *Thin-Walled Struct.*, Vol. 12, No. 3, pp. 229-263 (1991).

Corona, E., and Kyriakides, S., "Asymmetric Collapse Modes of Pipes under Combined Bending and Pressure," *Int. J. Solids Struct.*, Vol. 24, No. 5, pp. 505-535 (2000).

Corona, E., Lee, L.H., and Kyriakides, S., "Yield Anisotropic Effects on Buckling of Circular Tubes under Bending," *Int. J. Solids Struct.*, Vol. 43, No. 22, pp. 7099-7118 (2006).

Elchalakani M., and Zhao X.L., "Concrete-filled Cold-formed Circular Steel Tubes Subjected to Variable Amplitude Cyclic Pure Bending," *Eng. Struct.*, Vol. 30, No. 2, pp. 287-299 (2008).

Elchalakani, M., Zhao, X.L., and Grzebieta, R.H., "Plastic Mechanism Analysis of Circular Tubes under Pure Bending," *Int. J. Mech. Sci.*, Vol. 44, No. 6, pp. 1117-1143 (2002).

Guo, L., Yang, S., and Jiao, H., "Behavior of Thin-walled Circular Hollow Section Tubes Subjected to Bending," *Thin-Walled Struct.*, Vol. 73, pp. 281-289 (2013).

Houliara, S., and Karamanos, S.A., "Buckling and Post-buckling of Long Pressurized Elastic Thin-walled Tubes under In-plane Bending," *Int. J. Nonlinear Mech.*, Vol. 41, No. 4, pp. 491-511 (2006).

Jiao, H., and Zhao, X.L., "Section Slenderness Limits of Very High Strength Circular Steel Tubes in Bending," *Thin-Walled Struct.*, Vol. 42, No. 9, pp. 1257-1271 (2004).

Lee, K.L., "Mechanical Behavior and Buckling Failure of Sharp-notched Circular Tubes under Cyclic Bending," *Struct. Eng. Mech.*, Vol. 34, No. 3, pp. 367-376 (2010).

Lee, K.L., Hsu, C.M., and Pan, W.F., "Viscoplastic Collapse of Sharp-notched Circular Tubes under Cyclic Bending," *Acta Mech. Solida Sinica*, Vol. 26, No. 6, pp. 629-641 (2013).

Lee, K.L., Hung, C.Y., and Pan, W.F., "Variation of Ovalization for Sharp-notched Circular Tubes under Cyclic Bending," *J. Mech.*, Vol. 26, No. 3, pp. 403-411 (2010).

Lee, K.L., Pan, W.F., and Hsu, C.M., "Experimental and Theoretical Evaluations of the Effect between Diameter-to-thickness Ratio and Curvature-rate on the Stability of Circular Tubes under Cyclic Bending," *JSME Int. J., Ser. A*, Vol. 47, No. 2, pp. 212- 222 (2004).

Lee, K.L., Pan, W.F., and Kuo, J.N., "The Influence of the Diameter-to-thickness Ratio on the Stability of Circular Tubes under Cyclic Bending," *Int. J. Solids Struct.*, Vol. 38, No. 14, pp. 2401-2413 (2001).

Limam, A., Lee, L.H., and Kyriakides, S., "On the Collapse of Dented Tubes under Combined Bending and Internal Pressure," *Int. J. Solids Struct.*, Vol. 55, No. 1, pp. 1-12 (2012).

Pan, W.F., and Fan, C.H., "An Experimental Study on the Effect of Curvature-rate at Preloading Stage on Subsequent Creep or Relaxation of Thin-walled Tubes under Pure Bending," *JSME Int. J., Ser. A*, Vol. 41, No. 4, pp. 525-531 (1998).

Pan, W.F., and Her, Y.S., "Viscoplastic Collapse of Thin-walled Tubes under Cyclic Bending," *ASME J. Eng. Mat. Tech.*, Vol. 120, No. 4, pp. 287-290 (1998).

Pan, W.F., Wang, T.R., and Hsu, C.M., "A Curvature-ovalization Measurement Apparatus for Circular Tubes under Cyclic Bending," *Exp. Mech.*, Vol. 38, No. 2, pp. 99-102 (1998)

Shaw, P.K., and Kyriakides, S., "Inelastic Analysis of Thin-walled Tubes under Cyclic Bending," *Int. J. Solids Struct.*, Vol. 21, No. 11, pp. 1073-1110 (1985).

Suzuki, N., Tajika, H., Igi, S., Okatsu, M., Kondo, J., and Arakawa, T., "Local Buckling Behavior of 48 High-strain Line Pipes," *Pro. of the 8th Int. Pipeline Conf.*, Alberta, Canada, ICP 2010-31637 (2010).

Yuan, W., and Mirmiran, A., "Buckling Analysis of Concrete-filled FRP Tubes," *Int. J. Struct. Stab. Dyn.*, Vol. 1, No. 3, pp. 367-383 (2001).

Zhi, X.D., Fan, F., and Shen, S.Z., Failure Mechanism of Single-layer Cylindrical Reticulated Shells under Earthquake Motion," *Int. J. Struct. Stab. Dyn.*, Vol. 12, No. 2, pp. 233-249 (2012).

NOMENCLATURE

a dent depth

C material parameter

C_o material parameter

D_o original outer diameter

L_o original tube length
M moment
M_o moment for normalization
N_b number of bending cycles required to produce buckling
N_f number of bending cycles required to produce failure
t wall-thickness
α material parameter
α_o material parameter
β material parameter
ΔD_o change in outer diameter
ε uniaxial strain
γ material parameter
κ curvature
κ_c cyclic controlled curvature
κ_o curvature for nomalization
θ half of the central angle
ρ radius of curvature
σ uniaxial stress

局部凹痕圓管之循環彎曲退化與失效

李國龍
遠東科技大學創新設計與創業管理系

鍾誠錚 潘文峰
國立成功大學工程科學系

摘 要

本文主要是實驗與理論研究局部凹痕 6061-T6 鋁合金圓管在循環彎曲負載下的退化及失效。我們使用一個很簡單的技術用來製作圓管上的縱向局部凹痕，而凹痕的深度分佈由很淺到幾乎壁厚的 2.4 倍。實驗結果顯示，隨著循環圈數的增加，橢圓化-曲率關係呈現棘齒狀的成長，且凹痕深度越深時，該關係就越不對稱，橢圓化增加也就越大。實驗雙對數座標的控制曲率-循環至失效圈數關係呈現，五種不同的凹痕深度對應出五條不平行的直線。最後，本研究使用有限元素模式來描述彎矩-曲率及橢圓化-曲率關係。此外，本研究也提出一個理論模式來描述控制曲率-循環至失效圈數關係，在與實驗結果比較後發現，理論能夠合理描述實驗結果。